

PAPER • OPEN ACCESS

Synthesis of the BiVO_4 nanoparticle as an efficient photocatalyst to activate hydrogen peroxide for the degradation of methylene blue under visible light irradiation

To cite this article: P T D Pham *et al* 2019 *IOP Conf. Ser.: Mater. Sci. Eng.* **479** 012036

View the [article online](#) for updates and enhancements.



IOP | ebooks™

Bringing you innovative digital publishing with leading voices to create your essential collection of books in STEM research.

Start exploring the collection - download the first chapter of every title for free.

Synthesis of the BiVO_4 nanoparticle as an efficient photocatalyst to activate hydrogen peroxide for the degradation of methylene blue under visible light irradiation

P T D Pham^{1, 2}, P Q T Bui², L X Nong¹, V H Nguyen¹, L G Bach¹, H T Vu³, H T Nguyen⁴, T D Nguyen^{1, 5}

¹ NTT Hi-Tech Institute, Nguyen Tat Thanh University, 300A Nguyen Tat Thanh Street, District 4, Ho Chi Minh City, Vietnam.

² Faculty of Chemical Technology, Ho Chi Minh City University of Food Industry, 140 Le Trong Tan Street, Tan Phu District, Ho Chi Minh City, Vietnam.

³ Faculty of Hydro-Meteorology, HCMC University of Natural Resources and Environment, Le Van Sy Street, Ward 1, Tan Binh District, Ho Chi Minh City, Vietnam.

⁴ Son La Hydro Power Company, No 56 Lo Van Gia Street, Group 3, Chieng Le Ward, Son La Province, Vietnam

⁵ E-mail: ndtrinh@ntt.edu.vn

Abstract. In this study, we investigated the synthesis of BiVO_4 nanoparticles via the hydrothermal method and their photocatalytic activity for the degradation of methylene blue (MB) under LED visible light mediated by H_2O_2 . The obtained BiVO_4 catalyst was characterized by XRD, Raman, SEM, and UV-vis DRS. The effect of H_2O_2 concentrate, pH, and MB initial concentration on the removal rate of MB was carefully studied. The results showed that MB was decolorized entirely after 30 min in the $\text{BiVO}_4/\text{H}_2\text{O}_2/\text{Vis}$ process whereas the decomposition rate of BiVO_4 with the absence of H_2O_2 is 78% after 60 min. The accelerated degradation of MB by in the $\text{BiVO}_4/\text{H}_2\text{O}_2/\text{Vis}$ process is due to H_2O_2 acts as the external electron acceptor, which could promote the separation of photo-induced electrons and holes.

1. Introduction

Bismuth vanadate (BiVO_4), with a bandgap energy of ca. 2.4 eV, has recently emerged as a promising semiconductor photocatalysis for application in the evolution of O_2 from water, conversion of CO_2 and degradation of organic dyes because it absorbs a substantial portion of the visible spectrum [1–3]. However, the efficiency achieved with BiVO_4 to date has been far below what is expected due to its poor electron-hole separation yield [4, 5].

Previous studies have reported that the photo-induced electron-hole pairs should be separated efficiently and transported to induce a photocatalytic reaction. Therefore, to enhance the photocatalytic activity, the synthesis of BiVO_4 with facilitating the separation of electron-hole pairs have been proposed. For example, BiVO_4 with a control over the morphology and crystallographic facets can enhance the photocatalytic performance [6–8]. The design of composite structure of the n-type (BiVO_4) a p-type semiconductor (e.g., TiO_2 , CdS, and SrTiO_3) could also improve the photocatalytic activity of BiVO_4 because the p-type semiconductor can act as the external electron acceptor, which can restrict



the recombination of electron and hole [9, 10]. Similarly, the formation of a p-n junction from the monoclinic scheelite phase of BiVO_4 to p-type tetragonal phase of BiVO_4 was recently investigated with significantly improving the photocatalytic activity of BiVO_4 [2, 10, 11].

The introduction of external electron acceptor is another essential and feasible strategy to enhance the performance of BiVO_4 photocatalyst. The presence of hydrogen peroxide (H_2O_2), potassium bromate (KBrO_3), persulfate (PS) and peroxymonosulfate (PMS) as electron acceptors can suppress the electron-hole pair, thus enhancing the photodegradation efficiency via generating more radical ($\cdot\text{OH}$, $\text{BrO}_2\cdot$ and $\text{SO}_4^{\cdot-}$) [12, 13].

Herein, we report the photocatalytic degradation of methylene blue (MB) over BiVO_4 under visible LED light irradiation. To improve the photocatalytic degradation of MB, a more stable H_2O_2 was added into the BiVO_4/Vis process. The recyclability of catalysts was conducted to measure its long-term applicability. We also investigated the effect of H_2O_2 concentrate, pH, and MB initial concentration on the removal rate of MB in detail.

2. Materials and methods

2.1. Synthesis of BiVO_4

BiVO_4 nanoparticles were prepared via hydrothermal method using $\text{Bi}(\text{NO}_3)_3$ (Sigma-Aldrich, 99%) and NH_4VO_3 (Sigma-Aldrich, 99%) as Bi and V source, respectively. Typically, four mmol of $\text{Bi}(\text{NO}_3)_3$ was added to 40 mL HNO_3 0.1 M under vigorous stirring to get a colorless solution (solution A). Four mmol of NH_4VO_3 was dissolved in 40 mL H_2O to get a clear yellow solution (solution B). Then, a yellow precipitate was formed immediately when the solution B was added to solution A. After stirring 1 h, the pH of the mixed solution was adjusted 5.0 using 0.2 M NaOH solution. The obtained solution was transferred into a 100 mL Teflon-lined stainless steel autoclave and heated at 160 °C for 24 h. After cooling naturally, the yellow precipitate was washed with water by centrifugation at 7000 rpm for 10 min five times and dried at 110 °C for 24 h followed by calcining at 400 °C for 3h.

2.2. Catalyst characterization

The XRD of BiVO_4 nanoparticles was carried out on a Bruker D8 Advance powder diffractometer with a $\text{Cu-K}\alpha$ excitation source and a scan rate of 0.02 °/s from 10° to 70°. Raman spectra were taken on a Raman spectrometer (Horiba Jobin Yvon) using a red laser (633 nm) as the excitation source. SEM was recorded on a Jeol instrument (JSM 7401F, Japan). UV-visible diffuse reflectance spectrum (UV-vis DRS) was recorded on a Shimadzu UV-vis spectrophotometer.

2.3. Photocatalytic test

The photocatalytic activity tests were conducted in a 250 ml double layer interbed interlayer glass beaker photocatalytic reactor under visible light irradiation using six white LED lamp (Cree L6, 10W, 1040 lm) at room temperature. The beaker was filled with a mixture of MB (100 mL), BiVO_4 sample (50 mg), and H_2O_2 . The pH value of the mixed solution was adjusted using 0.2 M NaOH or 0.2 M HCl solution, and then the suspension was magnetically stirred in the dark for 60 minutes to ensure adsorption-desorption equilibrium between MB and the surface of BiVO_4 before lighting on. During light irradiation, five ml of aliquots were withdrawn and immediately centrifuged to separate photocatalyst particles every 5 min. MB concentration was analyzed by a UV-visible spectrophotometer (Model Evolution 60S, Thermo Fisher Scientific) with the absorption intensity at its maximum absorbance wavelength of $\lambda = 664$ nm. To investigate effects of H_2O_2 concentration, pH, and MB concentration on photocatalytic activity of BiVO_4 , the H_2O_2 concentration was increased from 0 to 10^{-1} mol/L, and pH was increased from 3 to 9, whereas MB concentration was increased from 10 to 30 mg/L. In addition, we also investigated the effect of added anions, including NaCl (3 mM), Na_2SO_4 (3 mM), Na_2CO_3 (3 mM), and NaHCO_3 (3 mM), on photocatalytic activity of BiVO_4 .

3. Results and discussion

3.1. Characterization of the as-synthesized BiVO_4

Figure 1(A) shows the XRD patterns of the as-obtained BiVO_4 products obtained by hydrothermal method at 140 °C for 24 h. It is apparent that the XRD peaks of BiVO_4 can be well indexed to the scheelite-type monoclinic phase (JCPDS card no. 14-00688) [1, 2, 14]. In addition, characteristic peaks of bismuth oxide and vanadate oxide or impurities were not detected in the XRD patterns of BiVO_4 , implying that the BiVO_4 catalyst was high purity and single-phase. The mean size crystalline BiVO_4 (τ , nm) was calculated based on the Scherrer equation [15]:

$$\tau = \frac{K\lambda}{\beta \cos \theta}$$

where, K is constant (0.9), λ is the X-ray wavelength (0.15405 nm), β is the line broadening at half the maximum intensity (FWHM, radians), and θ is the Bragg angle. The mean size crystalline BiVO_4 obtained from XRD data is 30.2 nm.

To provide more structural information, Raman analysis was conducted. The Raman spectra of the BiVO_4 catalyst is presented in Figure 1(B). As shown in Figure 1(B), the strongest band at 830 cm^{-1} is attributed to the symmetric V–O stretching mode, while the peaks at 641 cm^{-1} and 709 cm^{-1} are due to the asymmetric stretching mode of V–O bonds. The Raman peak at 324 cm^{-1} and 367 cm^{-1} are assigned to the asymmetric and symmetric deformation mode of VO_4^{3-} , respectively. The external modes (i.e., crystal lattice translational and rotational modes) of BiVO_4 were observed at 130 cm^{-1} and 212 cm^{-1} . Besides, based on the Raman shift of the V–O bond (ν , cm^{-1}), we calculate the V–O bond length of BiVO_4 (R , Å) by using the empirical expression: $\nu = 21349 \cdot e^{-19176 \cdot R}$ [16]. The V–O bond length using the empirical expression was 1.693 Å, which is consistent with the V–O bond length in monoclinic scheelite phase of BiVO_4 crystal. Raman result, along with XRD result, indicates that BiVO_4 crystal with single monoclinic scheelite phase was successfully prepared by hydrothermal method.

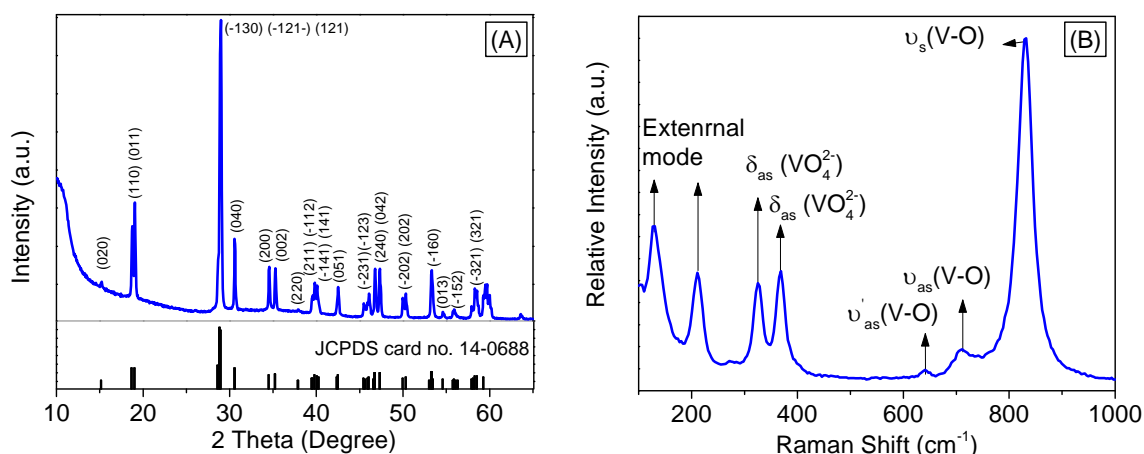


Figure 1. XRD pattern (A) and Raman spectra (B) of BiVO_4 sample.

The morphologies of BiVO_4 was investigated by SEM, as shown in Figure 2 A and B. It is seen that the as-synthesized BiVO_4 consists of cocoon-shaped particles, which was further confirmed by TEM result (Figure 2 C). The length and width of the cocoon-like particles is about 100~250 nm and 50~100 nm, respectively. This result has a difference from the mean size calculated by the Sherrer equation due to the clustering of particles.

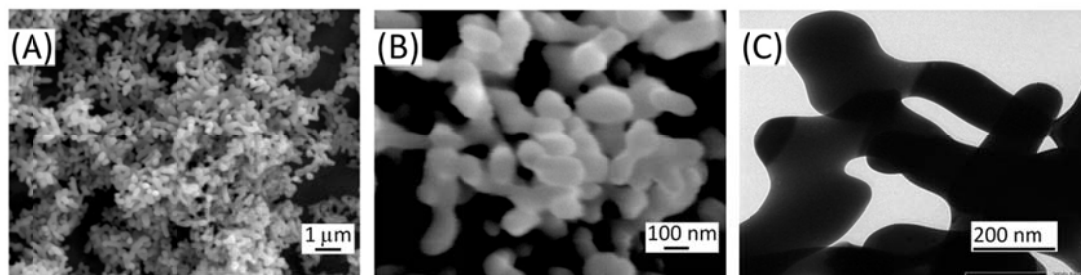


Figure 2. SEM images (A and B) and TEM image (C) of BiVO₄ sample.

UV-Vis DRS of the as-synthesized BiVO₄ sample in comparison with TiO₂-P25 is plotted in Figure 3(A). As comparison to TiO₂, BiVO₄ exhibited strong absorption in visible light range, which can facilitate the enhancement of photocatalytic activity of the BiVO₄ catalysts under the visible light irradiation. The indirect band gap energy (E_g) was evaluated using the relation: $(\alpha h\nu)^2 = A(h\nu - E_g)$, wherein A was the absorption coefficient near the absorption edge, h was the Planck constant (eV), and α was a constant [2,17]. The plot of function $(\alpha h\nu)^2$ plots versus photon energy ($h\nu$) of BiVO₄ sample is shown in Figure 3(B). The estimated band gap value is 2.39 eV, which is in a good agreement with previous studies [2,11,17].

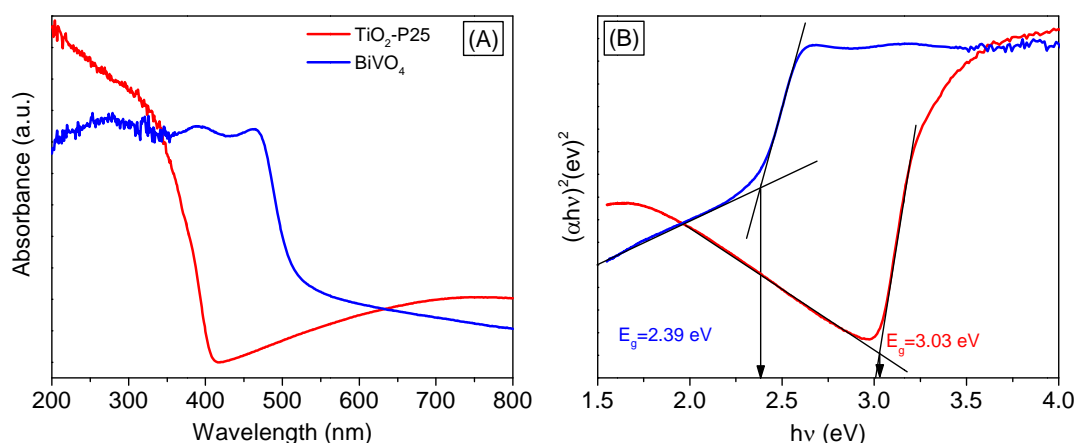


Figure 3. UV-vis DRS spectra (a) and estimated band gap (b) of BiVO₄ sample.

3.2. Photocatalytic performance

MB was degraded using BiVO₄ photocatalyst with the presence of H₂O₂ under white LED light. Typical results are present in Figure 4(A). The degradation of MB with irradiation only and the H₂O₂/Light system was not improved, indicating that H₂O₂ could not be activated by visible light irradiation. The photodegradation of MB with single BiVO₄ ([H₂O₂] = 0 M) is 78% after 60 min of irradiation, whereas the degradation rate with the BiVO₄/H₂O₂/light system ([H₂O₂] = 10⁻³ M) increases to 96% after 15 min of irradiation. BiVO₄ exhibited the poor photocatalytic activity is due to its poor charge transport characteristics and weak surface adsorption, therefore, facilitate the recombination of excessive electrons and hole [3,12,14,18]. A comparison in the photocatalytic properties with the benchmark material used in this study (TiO₂-P25) will be performed. With the presence of H₂O₂ as the acceptor electron, this recombination was restricted, resulting the photocatalytic performance was improved. The possible photocatalytic mechanism for BiVO₄ with the presence of H₂O₂ under visible light irradiation was represented as follows [12]:





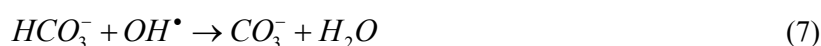
The HO^\bullet radical was known as a strong oxidizer, and therefore the formation rate of HO^\bullet radicals has a good correlation with the photocatalytic activity [1,11,19]. The time evolution of the spectral changes during the photodegradation of MB over $BiVO_4$ with the absence and presence of H_2O_2 under white LED light was shown in Figure 4(E) and (F), respectively. With the prolongation of the irradiation time, the intensities of the MB absorption peaks at 664 nm gradually decrease, and the color of the solution faded, which was due to the destruction of the MB with the chromophoric structure [20].

As also displayed in Figure 4(A), the increase added H_2O_2 concentration is favorable to enhancement degradation rate. However, when H_2O_2 was adjusted to 10^{-6} M, the MB removal rate was not improved because of the insufficiency of the generated HO^\bullet . When increasing the added H_2O_2 concentration to 10^{-1} M, the degradation rate also decreased.

Figure 4(B) displayed the effect of initial pH on the photodegradation degree of MB in the $BiVO_4/H_2O_2$ /Light system with H_2O_2 concentration fixing at 10^{-3} M. The result showed that no significant difference is observed in the MB photodegradation degree within the tested reaction period of 60 min in the lower initial pH levels (pH = 3–5). However, when the solution pH was increased to 7 and 9, the lower conversions were observed. The lower performance of the $BiVO_4/H_2O_2$ /Light system is due to H_2O_2 became highly unstable and was decomposed into water and oxygen under an alkaline pH [12]. While H_2O_2 act as an oxidant and most importantly the source of HO^\bullet in the $BiVO_4/H_2O_2$ /Light process.

To investigate the effect of initial MB concentration on the photocatalytic decomposition of MB, the photocatalytic tests were performed in varying concentration from 10 to 30 mg/L. The results (Figure 4C) indicated that the photodegradation degree was reduced with the increased initial MB concentration, while keeping a fixed amount of $BiVO_4$, H_2O_2 concentration and pH value of solution. This decrease is due to the decrease the OH radical formed on the interface of the catalyst/water during irradiation. With an increase of initial MB concentration corresponding to an increase of adsorbed organic substances on the surface of $BiVO_4$, the number of photons which are available to reach the catalyst surface was inhibited, and therefore less $\bullet OH$ are formed.

In Figure 4(D) we have presented the influence of anions such as NaCl, Na_2SO_4 , $NaHCO_3$, and Na_2CO_3 on the photocatalytic activity of $BiVO_4$. With the presence of NaCl and Na_2SO_4 , no significant difference is observed in the MB photodegradation degree. By contrast, $NaHCO_3$ and Na_2CO_3 could inhibit the photodegradation significantly. It may be due to the reaction of these anions with HO^\bullet (see reaction (6) and (7)), resulting in prolonged MB removal [12]. NaCl and Na_2SO_4 can react with $h_{\nu B}^+$ (reaction 8 and 9) [21].



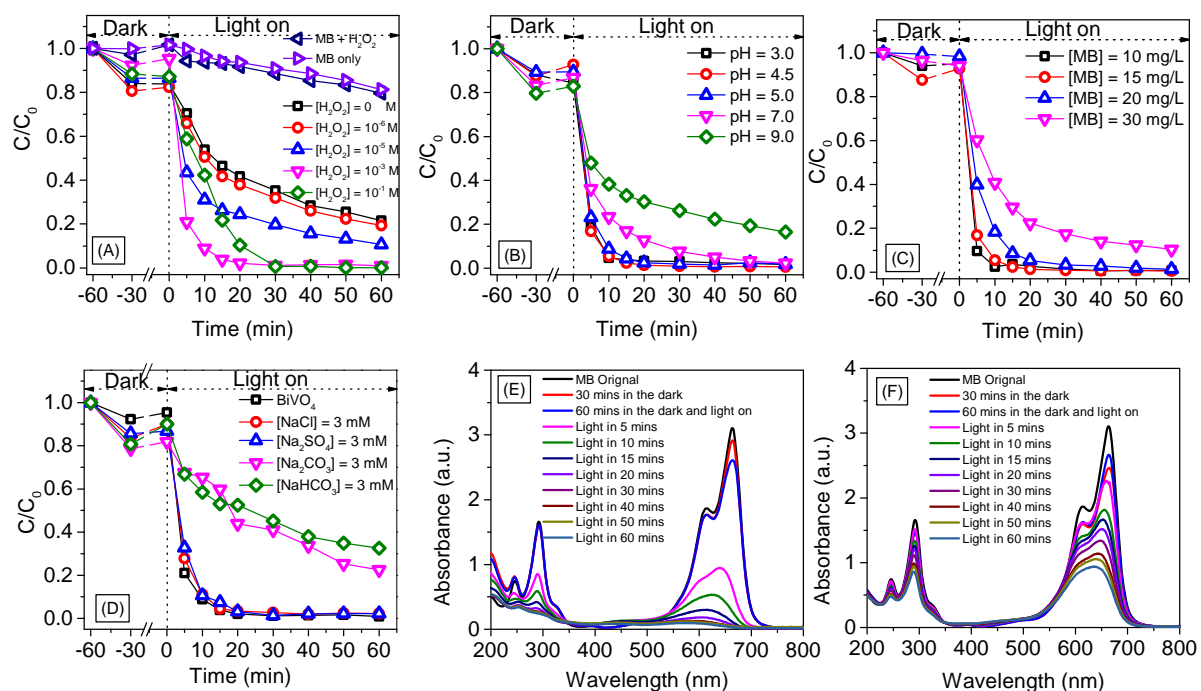


Figure 4. Effect of concentration of H_2O_2 (A), the initial pH (B), the initial concentration of MB (C), and anions (D) on photocatalytic degradation efficiency of MB over $BiVO_4$ and UV-vis absorption spectra of MB solution separated from catalyst suspension during illumination using $BiVO_4$ in the absence of H_2O_2 (E) and the presence of H_2O_2 (F).

3.3. The repeatability of photocatalyst activity

The recyclability of catalysts is essential properties for practical applications. The photocatalytic test of $BiVO_4$ was repeated five-time. It is seen that the photocatalytic performance did not significantly reduce after five successive runs (Figure 5). The MB photodecomposition level kept on higher than 90% in each run. This result indicated that $BiVO_4$ was not corroded and rather stable in the during the photocatalytic test.

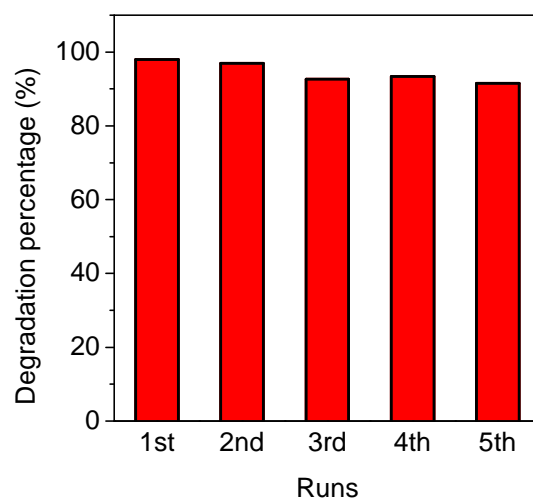


Figure 5. Cycling runs in the photocatalytic degradation of MB in the $BiVO_4/H_2O_2/Vis$ process.

4. Conclusions

We successfully synthesized BiVO₄ photocatalytic with a bandgap energy of ca. 2.39 eV by hydrothermal method and applied for photocatalytic degradation of MB under the visible LED light. MB was decolorized entirely after 30 min in the BiVO₄/H₂O₂/Vis process whereas the decomposition rate of BiVO₄ with the absence of H₂O₂ is 78% after 60 min. The accelerated degradation of MB by the BiVO₄/H₂O₂/Vis process is due to H₂O₂ acts as the external electron acceptor, which could restrict the recombination of photoinduced electrons and holes. Moreover, the as-prepared BiVO₄ sample exhibited reasonable good reusability and stability after five-time reaction recycles.

Acknowledgments.

This research is funded by the National Foundation for Science and Technology Development (NAFOSTED), Vietnam, under grant No.104.05-2017.315.

References

- [1] Ge M, Liu L, Chen W, Zhou Z 2012 *Cryst. Eng. Comm.* **14** 1038–1044
- [2] Nguyen D T, Hong S S 2017 *Top. Catal.* **60** 782–788
- [3] Zhang Y, Guo Y, Duan H, Li H, Sun C & Liu H 2014 *Phys. Chem. Chem. Phys.* **16** 24519–24526
- [4] Pingmuang K, Chen J, Kangwansupamonkon W, Wallace G G, Phanichphant S & Nattestad A 2017 *Sci. Rep.* **7** 8929
- [5] Zou L, Wang H, Wang X 2017 *ACS Sustain. Chem. Eng.* **5** 303–309
- [6] Tan H L, Wen X, Amal R, Ng Y H 2016 *J. Phys. Chem. Lett.* **7** 1400–1405
- [7] Chen L, Wang J, Meng D, Xing Y, Wang C, Li F, Wang Y & Wu X 2015 *Mater. Lett.* **147** 1–3
- [8] Tan G, Zhang L, Ren H, Huang J, Yang W, Xia A 2014 *Ceram. Int.* **40** 9541–9547
- [9] Petala A, Bontemps R, Spartatouille A, Frontistis Z, Antonopoulou M, Konstantinou I, Kondarides D I & Mantzavinos D 2017 *Catal. Today.* **280** 122–131
- [10] Usai S, Obregón S, Becerro A I & Colón G 2013 *J. Phys. Chem. C.* **117** 24479–24484
- [11] Yan M, Yan Y, Wu Y, Shi W & Hua Y 2015 *RSC Adv.* **5** 90255–90264
- [12] Lai H F, Chen C C, Chang Y K, Lu C S & Wu R J 2014 *Sep. Purif. Technol.* **122** 78–86
- [13] Xu T, Zhu R, Zhu G, Zhu J, Liang X, Zhu Y & He H 2017 *Appl. Catal. B Environ.* **212** 50–58
- [14] Ma Y, Jiang H, Zhang X, Xing J & Guan Y 2014 *Ceram. Int.* **40** 16485–16493
- [15] Nguyen D T & Hong S S 2017 *J. Nanosci. Nanotechnol.* **17** 2690–2694
- [16] Frost R L, Henry D A, Weier M L & Martens W 2006 *J. Raman Spectrosc.* **37** 722–732
- [17] Cooper J K, Gul S, Toma F M, Chen L, Liu Y S, Guo J, Ager J W, Yano J & Sharp I D 2015 *J. Phys. Chem. C.* **119** 2969–2974
- [18] Xi G & Ye J 2010 *Chem. Commun.* **46** 1893
- [19] Yu J, Wang W, Cheng B & Su B L 2009 *J. Phys. Chem. C.* **113** 6743–6750
- [20] Cesano F, Rahman M M, Bardelli F, Damin A & Scarano D 2016 *ChemistrySelect.* **1** 2536–2541
- [21] Konstantinou I K & Albanis T A 2004 *Appl. Catal. B Environmental.* **49** 1–14